

Electroluminescence and charge storage characteristics of quantum confined germanium nanocrystals

S. Das,¹ R. K. Singha,¹ A. Dhar,¹ S. K. Ray,^{1,a)} A. Anopchenko,² N. Daldosso,² and L. Pavesi²

¹*Department of Physics and Meteorology, Indian Institute of Technology Kharagpur, Kharagpur 721302, India*

²*Laboratorio di Nanoscienze, Dipartimento di Fisica, Università di Trento, Via Sommarive 14, 38100 Povo (Trento), Italy*

(Received 31 May 2011; accepted 3 June 2011; published online 28 July 2011)

Quantum confined Ge nanocrystals embedded in high bandgap and high-k Al₂O₃ dielectric matrix have been synthesized to demonstrate dual functional devices using Si-compatible fabrication technology. Transmission electron microscopy has shown the formation of Ge nanocrystals of varying diameter from 2.5 to 7.5 nm, much lower than the excitonic Bohr radius of Ge. A broad visible electroluminescence band at room temperature has been observed, which is attributed to the recombination of injected electrons and holes in Ge nanocrystals. An anti-clockwise hysteresis in the capacitance-voltage measurement of these devices indicates the charge storage in nanocrystals, useful for floating gate memory devices. © 2011 American Institute of Physics. [doi:10.1063/1.3610396]

I. INTRODUCTION

Multifunctional electronic devices integrate more electronic functions in a single device. Metal-oxide-semiconductor (MOS) structures embedded with nanocrystals (NCs) are attractive for dual function applications, as in light emitting diodes (LEDs) and floating gate memory devices. In dual function application, two electronic devices are merged into one device, and an electronic device system can be simplified. Light emitting memory devices, a class of multifunctional devices integrating a light source with a traditional flash memory transistor, show several applications in highly integrated optoelectronic devices. Walters *et al.*¹ demonstrated a field effect driven electroluminescence (EL) by excitonic emission from Si NCs which are embedded in a gate oxide. An alternating current (ac) voltage is applied at the gate electrode of a metal oxide semiconductor (MOS) transistor device in order to charge the Si NCs in sequence with electrons and holes. In that way, both charge carriers are injected from the transistor channel via Fowler–Nordheim (FN) tunneling through the oxide barrier. The excitons formed in the Si NCs recombine radiatively; the emitted wavelength depends on the NC size. In floating gate devices, semiconductor nanocrystals are the charge-storage nodes placed in the gate oxide between the gate and the channel.^{1–6} As a result of the smaller bandgap, superior carrier mobilities, and higher excitonic Bohr radius compared to Si,⁷ Ge-NCs are considered to be ideal for memory devices. CMOS compatibility of Ge has been already demonstrated in high-frequency amplifiers. On the other hand, efficient light emission from Ge nanostructures is desired for high-bandwidth intra-chip and inter-chip optical interconnects.⁸ Ge-NC in a SiO₂ matrix exhibits efficient photoluminescence (PL), which can be tuned by changing the size of the

nanocrystals.^{9,10} The origin of photoluminescence in Ge-NC is still under debate,^{7,11,12} owing to the presence of oxide defects and nanocrystal interfaces. Therefore, the attainment of band-edge or energy quantized electroluminescence in an indirect bandgap semiconductor is essential for the fabrication of nanocrystal light emitting devices. However, there are only few reports on Ge-NC based electroluminescent devices due to the problematic carrier injection in Ge-NCs.^{13,14}

In this paper, we report the fabrication of novel dual functional light emitting metal-insulator-semiconductor (MIS) flash memory structures by pulsed laser deposition (PLD) of Ge-NC in a high-k Al₂O₃ matrix. Compared to hafnium oxide, alumina exhibits a high thermal stability and remains in the amorphous phase even after annealing at > 1000 °C. In addition, to improve the charge retention properties of the non-volatile memory devices, Al₂O₃ with a larger bandgap (6.8 eV)¹⁵ is preferable compared to HfO₂ (5.8 eV).¹⁶ The charge injection into confined nanocrystals exhibiting light emission in the visible wavelength range at room temperature and the charge storage behavior of an Al/Al₂O₃(Ge-NC)/SiO₂/Si MIS structure have been studied.

II. EXPERIMENTAL

The light emitting memory structure was formed by a MIS capacitor with a dielectric stack consisting of Ge-NC embedded in Al₂O₃ sandwiched between SiO₂ tunneling and Al₂O₃ capping layers. The process starts with the thermal growth at 900 °C of a SiO₂ tunneling layer of thickness 4–5 nm on a chemically cleaned p-type Si(001) wafer of resistivity 7–14 Ω-cm, followed by the PLD deposition of 4 nm thick Ge-rich Al₂O₃. A pulsed KrF excimer laser (1.5 J/cm² energy density, 248 nm wavelength, and 25 ns pulse length) was used to ablate the Ge (99.999%) and Al₂O₃ targets placed on a rotating holder inside a vacuum chamber pumped down to 10^{–6} Torr. Finally, a 27 ± 1 nm thick Al₂O₃ cap layer was

^{a)}Author to whom correspondence should be addressed. Electronic mail: physkr@phy.iitkgp.ernet.in.

deposited. A control sample was deposited with the same conditions but without Ge. The samples were annealed in nitrogen at 850 °C (referred to as sample PGN850) or at 950 °C (referred to as sample PGN950) for 30 min. The process ended with the evaporation of the Al top and bottom contacts. The thin semi-transparent Al-gate top electrode has an area of $1.96 \times 10^{-3} \text{ cm}^2$ which defines the active area of the device. High-resolution transmission electron microscopy (HRTEM) was carried out using a JEM 2100 F (JEOL) system with an operating voltage of 200 kV to probe the formation of Ge nanocrystals. The electrical properties of the samples were measured by a Keithley semiconductor parameter analyzer (4200-SCS). The electroluminescence signals were collected with a Spectra-Pro 2300i monochromator coupled with nitrogen cooled charge-coupled device (CCD) camera. The total light intensity was calculated by integrating the CCD camera signal over the illuminated pixels.

III. RESULTS AND DISCUSSION

A. TEM studies

Figures 1(a) and 1(b) show the plane-view TEM images of Ge-NC embedded in Al_2O_3 for the PGN850 and PGN950

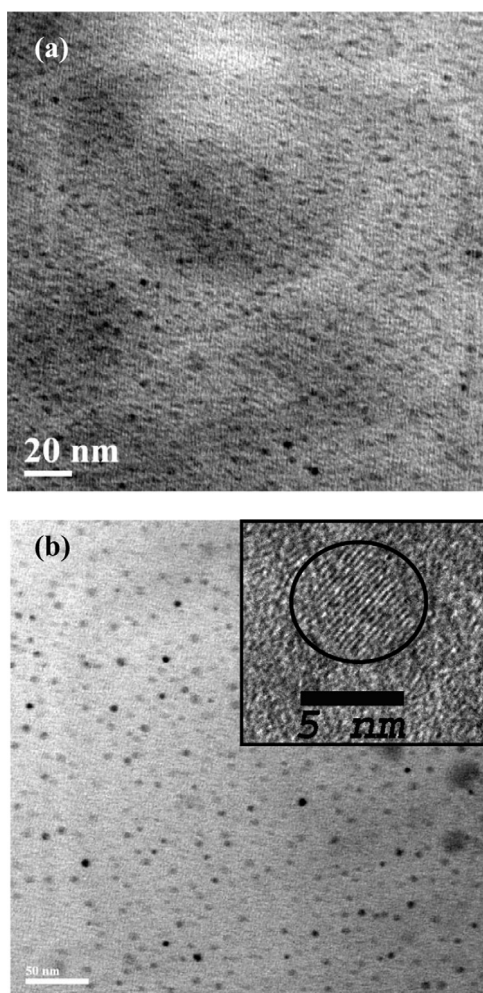


FIG. 1. Plane-view TEM micrographs of Ge-NC embedded in Al_2O_3 : (a) for 850 °C (PGN850) and (b) for 950 °C (PGN950) annealed samples. Dark patches are NCs. Inset of Fig. 1(b) shows the lattice fringes of one such NC.

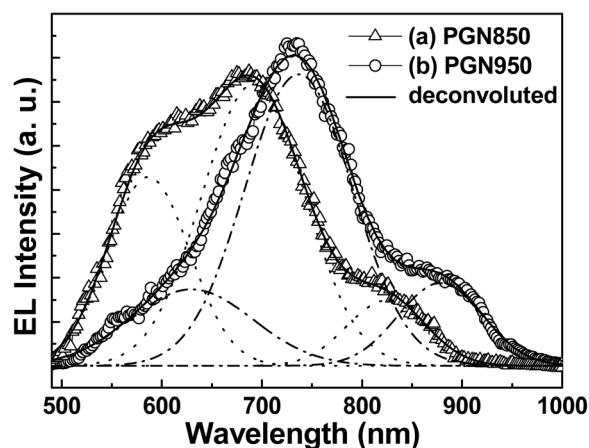


FIG. 2. Room temperature EL spectra of PGN850 and PGN950 devices.

samples, respectively. The nanocrystals are almost spherical and are homogeneously dispersed in the Al_2O_3 matrix. The inset of Fig. 1(b) shows lattice fringes with a separation of 0.33 nm, which corresponds to the $\{111\}$ plane of Ge with a diamond structure. Gaussian distributions with average sizes of 3.0 and 6.1 nm and full widths at half maximum (FWHM) of 1.1 and 1.9 nm are found for PGN850 and PGN950, respectively. These findings correlate well with what has been already reported for Ge-NC in SiO_2 .^{17,18}

B. Electroluminescence characteristics

Figure 2 reports the electroluminescence (EL) spectra of PGN850 and PGN950 devices for the injection currents 0.89×10^{-3} and 7.5×10^{-5} A. For PGN850 device (triangles), the EL spectrum can be fitted by three Gaussian peaks centered at 586, 691, and 824 nm with FWHM of 81, 102, and 78 nm, respectively. Similarly, the EL spectra of PGN950 device (circles) may be attributed to three peaks centered at 629, 736, and 878 nm with FWHM 122, 107, and 84 nm, respectively. The Gaussian peaks are blue shifted in the device with small Ge-NC, as predicted by quantum confinement models. The presence of more than one EL peak can be either due to the size distribution of the Ge-NC or to different recombination mechanisms. In particular, if the later hypothesis is valid, one can tentatively assign the most intense EL peak at 691 nm (736 nm) to electron-hole recombination in Ge-NC in Al_2O_3 , the weaker EL peak at 586 nm (629 nm) to defect related recombination at the Ge-NC/ Al_2O_3 interfaces,^{14,15} and the very weak peak at 824 nm (878 nm) to oxygen related defects in GeO_2 .

Figure 3 shows the integrated EL (I_{EL}) as a function of the current density (J). The onset voltage for EL emission has been found to be 3.7 and 14.4 V for PGN950 and PGN850, respectively. The lower onset voltage for the PGN950 device is due to the higher tunneling current as compared to PGN850 sample. This observation of size-dependent tunneling current agrees with the results reported for Si-NCs.¹⁹ The sample PGN950 has larger power efficiency than PGN850. It appears that injection and recombination are less effective in the smaller sized Ge-NC than in the

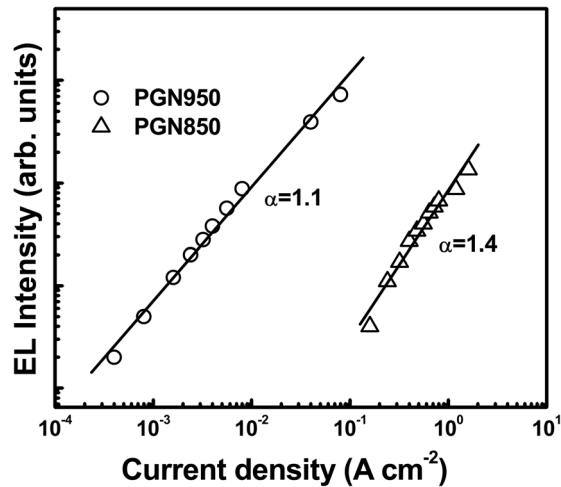


FIG. 3. Integrated EL intensity as a function of current density for the PGN850 and PGN950 light emitting memory devices.

larger ones. A power law characteristic is observed in Fig. 3 for the I_{EL} - J dependence, where

$$I_{EL} \sim J^\alpha. \quad (1)$$

The power law exponent α is 1.1 ± 0.1 for PGN950 and 1.4 ± 0.1 for PGN850. The larger α value for PGN850 points to a larger defect density for PGN850 than for the PGN950 sample.

There are two main mechanisms for Ge-NC excitation: (i) unipolar tunneling of hot electrons followed by impact ionization of the Ge-NC,²⁰ and (ii) bipolar tunneling of electrons and holes in the same Ge-NC.¹⁹ Since electroluminescence was only observed under forward bias (accumulation mode), we discard the impact excitation as the mechanism responsible for the emission. In fact, if this were the case, EL should be observed for both bias conditions, as electrons can be injected for both voltage polarities. On the contrary, holes can be injected only in forward bias when we observe electroluminescence.

Figure 4 shows the photoluminescence (PL) spectrum of a PGN950 sample at room temperature using an Ar laser

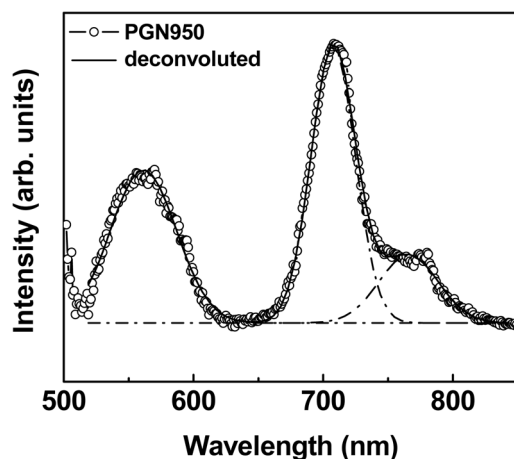


FIG. 4. Room temperature photoluminescence spectrum of PGN950 sample.

(wavelength 488 nm) as the excitation source. For the 850 °C annealed sample, we have not observed any significant PL signal, which may be due to the presence of non-radiative recombination centers in the lower temperature annealed sample. The PL spectrum is represented by three peaks centered at 561 nm, 708 nm, and 766 nm having FWHM of 51, 34, and 46 nm, respectively. It is noteworthy that the PL features are more resolved than the features observed in EL. By comparison with EL, the main peak at 708 nm in PL is attributed to exciton recombination in Ge-NC. By using a simple quantum confinement model,⁷ this transition energy corresponds to recombination in 6.6 nm Ge-NC, which closely matches the value observed by TEM. A 30 nm red-shift with respect to the main EL peak (736 nm, Fig. 2) is not surprising because of the different excitation conditions. Similar shifts in the literature have been attributed to quantum confined stark effects in the EL measurement.²¹ The other spectral features observed in PL do not correlate with the EL observations.

C. Charge storage characteristics

Figure 5 reports the high frequency (100 kHz, ± 10 V) capacitance–voltage (C–V) hysteresis behavior of the MIS structures for the control and the two Ge-NC rich samples. A small flat-band voltage shift of 0.17 V is observed for the control sample. On the contrary, large memory windows of 4.86 and 1.25 V are observed for the PGN950 and PGN850 samples, respectively. This suggests that the hysteresis is not due to traps in Al_2O_3 but instead to charges trapped in Ge-NC or at their interfaces. A flatband voltage shift of 4.86 V (1.25 V) obtained for the PGN950 (PGN850) sample gives rise to a stored charge surface density (N_{charge}) of $7.9 \times 10^{12} \text{ cm}^{-2}$ ($1.2 \times 10^{12} \text{ cm}^{-2}$).² It is observed that a device with larger size Ge-NC can store more charges. The inset of Fig. 5 shows the retention characteristics of the devices at room temperature. At first, the memory capacitor was programmed/erased under a drive gate voltage of +10 V/–10 V for 2 s. Then, the flatband voltage (V_{FB}) was measured with

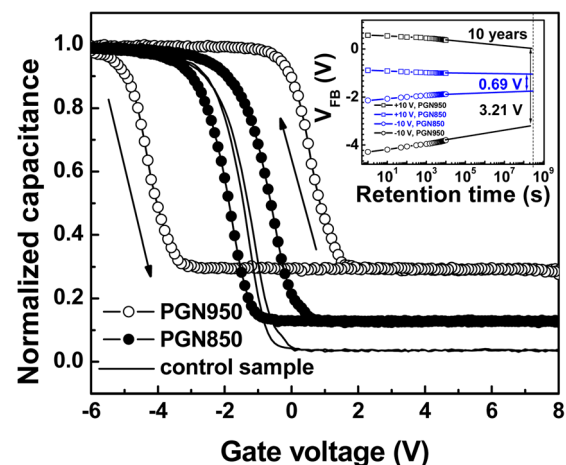


FIG. 5. (Color online) High-frequency (100 kHz) C–V characteristics of MIS capacitor for control sample and Ge nanocrystals in high- k Al_2O_3 matrix for PGN850 and PGN950 devices. Inset shows the charge retention characteristics of the trilayer memory devices annealed at different temperatures.

time. Assuming a logarithmic retention, a 10 year extrapolation of V_{FB} shift yields 3.20 V and 0.69 V for PGN950 and PGN850 samples, respectively, with estimated charge losses of 34% and 45%. This charge loss mechanism can be separated into two processes: (i) initial fast decay, which is due to lateral charge loss and the Coulomb repulsion between electrons confined in nanocrystals; and (ii) later slow decay, attributed to the leakage via tunneling barrier. It has been reported that for higher temperature annealed samples, the initial fast decay is suppressed due to the complete isolation of Ge nanocrystals²² in the oxide matrix. The high nanocrystal density and low inter-nanocrystal distance may give rise to comparatively higher lateral charge losses in 850 °C annealed samples.

IV. CONCLUSIONS

We have demonstrated dual function light emission and charge storage behavior using Ge nanocrystals embedded in a high bandgap and high-k Al_2O_3 oxide MIS structures. An intense electroluminescence at a wavelength of 691 and 736 nm from MIS devices having average Ge nanocrystal size of 3.0 and 6.1 nm, respectively, has been observed. Room temperature electroluminescence at low turn-on voltage shows that bipolar injection in Ge-NC is possible, when a low-energy barrier is used. An improved stored charge density, a large memory window, and a low charge loss of the Ge-NC memory device with high-k Al_2O_3 as a blocking oxide make this material system attractive for future high-density and scaled flash memory device applications.

ACKNOWLEDGMENTS

This work is supported by the ITPAR-DST Nanophotonics and DRDO FIR projects.

- ¹R. J. Walters, G. I. Bourianoff, and H. A. Atwater, *Nature Mater.* **4**, 143 (2005).
- ²H. I. Hanafi, S. Tiwari, and I. Khan, *IEEE Trans. Electron Devices* **43**, 1553 (1996).
- ³D. W. Kim, T. Kim, and S. K. Banerjee, *IEEE Trans. Electron Devices* **50**, 1823 (2003).
- ⁴K. Das, M. Nanda Goswami, R. Mahapatra, G. S. Kar, A. Dhar, H. N. Acharya, S. Maikap, J.-H. Lee, and S. K. Ray, *Appl. Phys. Lett.* **84**, 1386 (2004).
- ⁵S. Das, K. Das, R. K. Singha, A. Dhar, and S. K. Ray, *Appl. Phys. Lett.* **91**, 233118 (2007).
- ⁶D. Panda, A. Dhar, and S. K. Ray, *Semicond. Sci. Technol.* **24**, 115020 (2009).
- ⁷Y. Maeda, *Phys. Rev. B* **51**, 1658 (1995).
- ⁸M. Salib, L. Liao, R. Jones, M. Morse, A. Liu, D. Samara-Rubio, D. Alduino, and M. Paniccia, *Intel. Tech. J.* **8**, 143 (2004).
- ⁹S. Takeoka, M. Fujii, S. Hayashi, and K. Yamamoto, *Phys. Rev. B* **58**, 7921 (19998).
- ¹⁰K. Das, M. L. N. Goswami, A. Dhar, B. K. Mathur, and S. K. Ray, *Nanotechnology* **18**, 175301 (2007).
- ¹¹S. Das, R. K. Singha, S. Gangopadhyay, A. Dhar, and S. K. Ray, *J. Appl. Phys.* **108**, 053510 (2010).
- ¹²K. S. Min, K. V. Shcheglov, C. M. Yang, A. Atwater, M. L. Brongersma, and A. Polman, *Appl. Phys. Lett.* **68**, 2511 (1996).
- ¹³J.-Y. Zhang, Y.-H. Ye, X.-L. Tan, and X.-M. Bao, *Appl. Phys. A* **71**, 299 (2000).
- ¹⁴S.-T. Chang, S.-H. Liao, *J. Vac. Sci. Technol. B* **27**(1), 535 (2009).
- ¹⁵J. J. H. Gielis, B. Hoex, M. C. M. van de Sanden, and W. M. M. Kessels, *J. Appl. Phys.* **104**, 073701 (2008).
- ¹⁶S. Maikap, H. Y. Lee, T.-Y. Wang, P.-J. Tzeng, C. C. Wang, L. S. Lee, K. C. Liu, J.-R. Yang and M.-J. Tsai, *Semicond. Sci. Technol.* **22**, 884 (2007).
- ¹⁷H. Fukuda, T. Kobayashi, T. Endoh, and Y. Ueda, *Appl. Surf. Sci.* **130**, 776 (1998).
- ¹⁸W. K. Choi, V. Ho, V. Ng, Y. W. Ho, S. P. Ng, and W. K. Chim, *Appl. Phys. Lett.* **86**, 143114 (2005).
- ¹⁹A. Marconi, A. Anopchenko, M. Wang, G. Pucker, P. Bellutti, and L. Pavesi, *Appl. Phys. Lett.* **94**, 221110 (2009).
- ²⁰C. J. Lin and G. R. Lin, *IEEE J. Quantum Electron.* **41**, 441 (2005).
- ²¹Y.-H. Kuo, Y. K. Lee, Y. S. Ge, S. Ren, J. E. Roth, T. I. Kamins, D. A. B. Miller, and J. S. Harris, *Nature* **437**, 1334 (2005).
- ²²J. K. Kim, H. J. Cheong, Y. Kim, J. Y. Yi, and H. J. Park, *Appl. Phys. Lett.* **82**, 2527 (2003).